

# Predicting colloidal crystals from shapes via inverse design and machine learning

Yina Geng,<sup>1,\*</sup> Greg van Anders,<sup>1,\*</sup> and Sharon C. Glotzer<sup>1,2,3,4</sup>

<sup>1</sup>*Department of Physics, University of Michigan, Ann Arbor MI 48109, USA*

<sup>2</sup>*Department of Chemical Engineering, University of Michigan, Ann Arbor MI 48109, USA*

<sup>3</sup>*Department of Materials Science and Engineering, University of Michigan, Ann Arbor MI 48109, USA*

<sup>4</sup>*Biointerfaces Institute, University of Michigan, Ann Arbor MI 48109, USA*<sup>†</sup>

(Dated: October 26, 2021)

A fundamental challenge in materials design is linking building block attributes to crystal structure. Addressing this challenge is particularly difficult for systems that exhibit emergent order, such as entropy-stabilized colloidal crystals. We combine recently developed techniques in inverse design with machine learning to construct a model that correctly classifies the crystals of more than ten thousand polyhedral shapes into 13 different structures with a predictive accuracy of 96% using only two geometric shape measures. With three measures, 98% accuracy is achieved. We test our model on previously reported colloidal crystal structures for 71 symmetric polyhedra and obtain 92% accuracy. Our findings (1) demonstrate that entropic colloidal crystals are controlled by surprisingly few parameters, (2) provide a quantitative model to predict these crystals solely from the geometry of their building blocks, and (3) suggest a prediction paradigm that easily generalizes to other self-assembled materials.

A holy grail for materials researchers is the ability to predict crystal structures solely from knowledge about the constituent atoms, molecules, or particles, without the need for simulations or experiments. Many researchers have attempted this quest; a well-known example is the early effort of Pauling to predict crystal structures from atoms based solely on their atomic radii [1]. Pauling's rules have since been adopted to program the assembly of DNA-functionalized nanospheres into colloidal crystals isostructural to those Pauling considered for atoms, as well as ones with no atomic counterpart [2–5]. Prediction of crystals from molecules or anisotropic particles is substantially harder [6–8]. In 2012, a study of 145 different polyhedrally shaped particles and their entropy stabilized crystals provided sufficient data to discover a correlation between coordination number and isoperimetric quotient (IQ), a measure of the roundness of a particle [9]. The study found that knowledge of the coordination number in the dense fluid (a simple observable in simulations) and the particle IQ allows one to predict whether that fluid of particles will crystallize and, if so, whether it will form a liquid crystal mesophase, a medium-coordination crystal, or a close-packed crystal (including topologically close-packed phases). Despite being only partially predictive, that was the state of the art in 2012 and in the half dozen years since, despite continued discoveries of colloidal crystals that add to the knowledge base.

Here we leverage two recent important computational advances to enable a much higher level of predictiveness of colloidal crystal structures from particle shape. One advance is the inverse design methodology of digital alchemy [10, 11], a molecular simulation method in which particle attributes are treated as thermodynamic variables in a generalized, or extended, thermodynamic ensemble [12, 13]. Digital alchemy simulations produce optimal particle attributes for target thermodynamic phases, including complex colloidal crystals with

very large unit cells. [11] The other advance is the application of machine learning methods to materials problems. [14–19] Machine learning can discover hidden correlations in large datasets, providing clues to the long-sought relationship between building block and structure. By combining these two approaches to thermodynamic systems of hard, polyhedrally shaped particles, we find an empirical but highly predictive model for entropically ordered colloidal crystals from solely geometric measures of their constituent particles. Our model is capable of predicting 13 different entropically stable crystal structures formed by millions of different colloidal polyhedra with 96% fidelity using just two geometric measures of particle shape (see Fig. 1 for an illustration of our approach). With three measures, 98% fidelity is achieved. Though far from a first principles theory, this model can be used immediately to inform experiments and select building blocks for self-assembling nanoparticle superlattices and colloidal crystals.

To construct the predictive model we performed Alchemical Monte Carlo (Alch-MC) simulations based on the Digital Alchemy framework [10], using an implementation [11] that extends the Hard Particle Monte Carlo (HPMC) plugin [20] for HOOMD-Blue [21] to generalized thermodynamic ensembles that include particle shape change. We simulated  $NVT\mu$  ensembles at constant temperature  $T$ , fixed volume  $V$ , and chemical potential  $\mu = 0$  for 13 target structures reported previously in entropic self-assembly: simple cubic (SC), body-centered cubic (BCC), face-centered cubic (FCC), simple chiral cubic (SCC), hexagonal (HEX-1-0.6), diamond (D), graphite (G), honeycomb (H), body-centered tetragonal (BCT-1-1-2.4), high-pressure Lithium (Li),  $\beta$ -Manganese ( $\beta$ -Mn),  $\beta$ -Uranium ( $\beta$ -U), and  $\beta$ -Tungsten ( $\beta$ -W). The variable  $\mu$  is conjugate to the shape variable that is allowed to fluctuate in the simulation. We placed a minimum of  $N = 100$  particles in a periodic simulation box, with the exact number chosen to be a multiple of the number of particles in the unit cell of one of the 13 target structures. Particle shapes were initialized with as many as 64 vertices randomly generated to create a convex shape. Monte Carlo (MC) sweeps were performed to

\* These authors contributed equally to this work.

<sup>†</sup> grva@umich.edu, sglotzer@umich.edu

allow particle translations, rotations, and shape moves via vertex re-location. For each shape move, we (i) moved a vertex, (ii) resized the trial shape to unit volume, (iii) checked if the move induced any particle overlaps, and then (iv) accepted the move based on the Boltzmann factor as described in Ref. [10]. Translation and rotation moves followed standard procedures (see, e.g., Refs. [6, 7, 9, 22–25]).

We slowly compressed the target crystal structure comprised of a randomly generated shape to the target packing fraction, with springs of spring constant 1000 (where energy is specified in units of  $k_B T$  and length units are set by the particle size) at each node to maintain the integrity of the structure during the compression phase. In this initial stage, it is highly unlikely that the structure is thermodynamically stable, so fixing the positions of the centers of the particles over an initial set of MC steps allows the system to explore shape space during compression without falling apart. After reaching the target packing fraction, we logarithmically relaxed the spring constant to zero. We then further evolved the system at fixed packing fraction  $\eta$  for  $1 \times 10^6$  (BCC- $\eta = 0.6$ , FCC- $\eta = 0.6$ , SC- $\eta = 0.6$ , diamond- $\eta = 0.6$ , honeycomb- $\eta = 0.65$ , graphite- $\eta = 0.65$ , HEX-1-0.6- $\eta = 0.7$ , BCT-1-1-2.4- $\eta = 0.7$ , Li- $\eta = 0.65$ ) or  $2 \times 10^6$  (SCC- $\eta = 0.7$ ) or  $8 \times 10^6$  ( $\beta$ -W- $\eta = 0.6$ ) or  $3.6 \times 10^7$  ( $\beta$ -Mn- $\eta = 0.6$ ) or  $1 \times 10^8$  ( $\beta$ -U- $\eta = 0.6$ ) MC sweeps. For each target crystal structure, we performed 10 independent simulations and analyzed the shapes in the final  $5 \times 10^5$  sweeps. The output of the Alch-MC simulation procedure for each of the 13 crystal structures is a family of optimal shapes (that is, shapes that minimize the system free energy) with shape measures that fluctuate about some average value.

We calculated 10 measures of shape motivated by prior works studying the relationship between particle geometry and self-assembly behavior.[9] The shape measures calculated for each polyhedral shape are: the cosine of the average dihedral angle  $\theta_d$ ; the number of facets  $N_f$ ; the determinant of the moment of inertia  $I$ ; the trace of the moment of inertia; the ratio of the circumsphere radius to the insphere radius; IQ; the asphericity  $\alpha$ ; and the real and imaginary parts of the chiral parameter  $\chi$ . To calculate  $\cos \theta_d$ , facets with area  $a_f > a_f^*$  (we use  $a_f^* = 0.02$  but our results are not sensitive to changes in  $a_f^*$ ) were clustered by their normal vector using the DBSCAN [26] scikit-learn module [27]. Clustered facets are represented by area-weighted average normals. We computed the clustered-facets-area-weighted cosine of the angle between average normals of neighboring clustered facets in a polyhedron. The number of facets is the number of clustered facets using DBSCAN. The isoperimetric quotient  $IQ = 36\pi v^2/s^3$ , where  $v$  is the volume and  $s$  is the surface area of a polyhedron). The asphericity  $\alpha = Rs/3v$ , where  $R$  is the integrated mean curvature normalized by  $4\pi$ . Finally,  $\chi$  is the lowest order measure of the degree of chirality of a molecule [28] and it is zero for achiral molecules.  $\chi \propto \sum_{mn} C(234; mn) \rho_{2m} \rho_{3n} \rho_{4,m+n}^*$ ,

where  $C(234; mn)$  are the appropriate Clebsch-Gordan coefficients and  $\rho_{lm}$  are mass-weighted distance moments with  $\rho_{lm} = \sum_{\tau \in T} |\mathbf{r}_\tau|^l Y_{lm}(\theta_\tau, \phi_\tau)$ , where the sum is over atoms  $\tau$

in the molecule  $T$ . We calculated  $\chi$  for a polyhedron by assuming a unit mass atom at each vertex of its vertices.

Altogether, this procedure produced the dataset to be interrogated using machine learning (ML), with the aim of identifying salient geometric criteria for predicting structure. We utilized the random forest ML classification technique in scikit-learn. Random forest builds a large collection of decorrelated trees and then averages them to improve accuracy and control over-fitting. The technique is capable of high predictive accuracy and is applicable in high-dimensional problems such as this one with highly correlated variables. Here the 10 shape measures are provided as input and the 13 crystal structures as produced as output.

Table 1 reports correlations found for the  $\beta$ -Mn structure between the 10 tested geometric measures applied to 1000 free-energy minimizing shapes randomly selected from among the millions of shapes generated by the Alch-MC simulations. Tables reporting correlations for all other structures studied can be found in the Supplementary Materials, as Tables S1-S12. The ML analysis (see Fig. 2a) of low density data indicates that two shape features – ( $\text{Tr}(I)$ ) and ( $\langle \cos(\theta_d) \rangle$ ) — are the strongest predictors of the shape-structure relationship. Fig. 2c shows shape distributions for the 13 candidate structures using  $\text{Tr}(I)$  and  $\cos(\theta_d)$ .

The self-assembly of shapes that are now understood to be far from optimal [11] has been reported in the literature.[9, 23]. To develop a model that also correctly predicts assemblies for highly suboptimal shapes, we run additional simulations at other densities to broaden our data set. We further generate shape distributions at high densities with different number of shape vertices (FCC: number of vertices=32,  $\eta=0.65$ ; 32, 0.7; 32, 0.8; 32, 0.9; 32, 0.95; 32, 0.99; 10, 0.6; 12, 0.6; 14, 0.6; 20, 0.6; 50, 0.6; 120, 0.6; BCC: 6, 0.6; 14, 0.64), shape distributions are shown in Fig. S1. From this we find that distributions of particle shapes are clustered by geometry, and several structures exhibit multiple free energy basins. The existence of these basins indicates that for those structures multiple distinct particle shapes provide good candidate shapes for self-assembly.

We further note that shape distributions vary in form by structure. For example, G and H structures exhibit a narrow range of  $\cos(\theta_d)$  relative to the distributions for SC, SCC, BCC, BCT, and FCC. Conversely SC, SCC, BCC, BCT, and FCC all exhibit a narrow range of  $\text{Tr}(I)$  relative to the distributions for G and H. We expect that this relative sensitivity is an important consideration in the synthesis of appropriately shaped particles for self-assembly. Moreover, Fig. 2b shows regions that BCC, FCC,  $\beta$ -W,  $\beta$ -U, and  $\beta$ -Mn distributions locate tightly together in shape space with some overlap. The existence of this overlap accords with prior work [9] that found some hard polyhedra spontaneously self-assemble more than one structure (e.g.  $\beta$ -Mn and  $\beta$ -U).

Fig. 2d shows the two-parameter empirical model, obtained from the Alch-MC simulation data, that maps particle shape to structure. We also extracted thermodynamically optimal shapes from the peaks of the shape distributions in the two salient parameters. Fig. 3 shows peak positions, and inset particle images show representative particle shapes. Remarkably,

the two-parameter model predicts structure from shape with 96% accuracy. Inclusion of  $\alpha$  increases the accuracy of structure prediction to 98%.

As a further test of the model's predictive ability, we compared our model's predictions against the previously reported self-assembly behavior [9] of 81 known crystal-forming polyhedra, in which 71 shapes formed target structures included in our set of 13. Contained in that set are the cube [29, 30], truncated cube [29, 31], octahedron [29, 31], truncated octahedron [29], cuboctahedron [29], and rhombic dodecahedron [31], each of whose self-assembled colloidal crystal structures have been shown in experiments to match the simulated structures. In Ref. [9], shapes were self-assembled into crystals without the use of alchemical variables, and thus the shapes are not necessarily the optimal ones for the obtained crystal structure. For that reason, we expect the accuracy of our predictions to be lower than that obtained for optimal shapes. We found that the two-parameter model correctly predicts the crystal structure formed by 65 shapes in the 2012 study with a fidelity of 91.55%. The model is, of course, unable to correctly predict the structure for shapes that formed structures not included in our set of 13, and also failed to predict structures where multiple structures were reported. Model predictions and shapes are given in Fig. 4.

Our coupling of inverse design and machine learning techniques to create a purely geometric, two-parameter, empirical model that predicts the self assembly of colloidal crystals of convex polyhedra with a fidelity of 96% is a con-

siderable advance over the two-parameter, empirical model presented in Ref. [9]. Nevertheless, there is room for further improvement. First, our model was based on considering only 10 different shape features. It is possible that there are other shape features that could prove better predictors of self-assembly behavior. To facilitate investigations into this possibility, we have made raw shape data available online at [https://deepblue.lib.umich.edu/data/concern/generic\\_works/6q182k84r?locale=en](https://deepblue.lib.umich.edu/data/concern/generic_works/6q182k84r?locale=en). We encourage the community to use the data to look for increasingly accurate predictive models. Second, in regions of shape space that are either sparsely populated by our data and so yield poor statistics, or in which different structures are densely clustered, the model may fail to predict the correct structure. We encourage the community to add data to the online data set for additional shapes and structures beyond those considered here.

The fact that as few as two geometric criteria are sufficient to predict structure formation in crystals with as many as 30 ( $\beta$ -U) particles in a unit cell suggests that appropriate geometric criteria might be useful for predicting order in colloidal systems with other forces at play, including hydrogen bonding between DNA-programmable colloidal shapes, van der Waals attraction between ligands or between particle cores, depletion interactions, and so on. Alch-MC or other inverse design methods can treat any of these cases to produce optimized forces as well as shapes. Nevertheless, our predictions should extend to experimental systems of anisotropic colloids and nanoparticles in which entropy plays a major role.[6, 32]

- 
- [1] L. Pauling, *Journal of the American Chemical Society* **51**, 1010 (1929).
- [2] C. A. Mirkin, R. L. Letsinger, R. C. Mucic, and J. J. Storhoff, *Nature* **382**, 607 (1996).
- [3] R. J. Macfarlane, M. R. Jones, A. J. Senesi, K. L. Young, B. Lee, J. Wu, and C. A. Mirkin, *Angew. Chem., Int. Ed.* **49**, 4589 (2010).
- [4] F. Lu, K. G. Yager, Y. Zhang, H. Xin, and O. Gang, *Nature Communications* **6** (2015).
- [5] W. Liu, M. Tagawa, H. L. Xin, T. Wang, H. Emamy, H. Li, K. G. Yager, F. W. Starr, A. V. Tkachenko, and O. Gang, *Science* **351**, 582 (2016).
- [6] G. van Anders, D. Klotsa, N. K. Ahmed, M. Engel, and S. C. Glotzer, *Proc. Natl. Acad. Sci. U.S.A.* **111**, E4812 (2014), arXiv:1309.1187 [cond-mat.soft].
- [7] G. van Anders, N. K. Ahmed, R. Smith, M. Engel, and S. C. Glotzer, *ACS Nano* **8**, 931 (2014), arXiv:1304.7545 [cond-mat.soft].
- [8] H. Lin, S. Lee, L. Sun, M. Spellings, M. Engel, S. C. Glotzer, and C. A. Mirkin, *Science* **355**, 931 (2017).
- [9] P. F. Damasceno, M. Engel, and S. C. Glotzer, *Science* **337**, 453 (2012), arXiv:1202.2177 [cond-mat.soft].
- [10] G. van Anders, D. Klotsa, A. S. Karas, P. M. Dodd, and S. C. Glotzer, *ACS Nano* **9**, 9542 (2015), arXiv:1507.04960 [cond-mat.soft].
- [11] Y. Geng, G. van Anders, P. M. Dodd, J. Dshemuchadse, and S. C. Glotzer, (2017), arXiv:1712.02471 [cond-mat.soft].
- [12] A. Lyubartsev, A. Martsinovski, S. Shevkunov, and P. Vorontsov-Velyaminov, *The Journal of Chemical Physics* **96**, 1776 (1992).
- [13] J. Zhang, R. Blaak, E. Trizac, J. A. Cuesta, and D. Frenkel, *The Journal of Chemical Physics* **110**, 5318 (1999).
- [14] B. Meredig, A. Agrawal, S. Kirklin, J. E. Saal, J. W. Doak, A. Thompson, K. Zhang, A. Choudhary, and C. Wolverton, *Phys. Rev. B* **89**, 094104 (2014).
- [15] L. M. Ghiringhelli, J. Vybiral, S. V. Levchenko, C. Draxl, and M. Scheffler, *Phys. Rev. Lett.* **114**, 105503 (2015).
- [16] A. Agrawal and A. Choudhary, *APL Materials* **4**, 053208 (2016).
- [17] A. W. Long, C. L. Phillips, E. Jankowski, and A. L. Ferguson, *Soft Matter* **12**, 7119 (2016).
- [18] Y. Liu, T. Zhao, W. Ju, and S. Shi, *Journal of Materials* **3**, 159 (2017).
- [19] R. Ramprasad, R. Batra, G. Pilania, A. Mannodi-Kanakkithodi, and C. Kim, (2017), arXiv:1707.07294 [cond-mat.mtrl-sci].
- [20] J. A. Anderson, M. E. Irrgang, and S. C. Glotzer, *Comp. Phys. Commun.* **204**, 21 (2016).
- [21] J. A. Anderson and S. C. Glotzer, (2013), <http://codeblue.umich.edu/hoomd-blue>, arXiv:1308.5587 [physics.comp-ph].
- [22] A. Haji-Akbari, M. Engel, A. S. Keys, X. Zheng, R. G. Petschek, P. Palfy-Muhoray, and S. C. Glotzer, *Nature* **462**, 773 (2009), arXiv:1012.5138 [cond-mat.soft].
- [23] U. Agarwal and F. A. Escobedo, *Nat. Mater.* **10**, 230 (2011).
- [24] A. P. Gantapara, J. de Graaf, R. van Roij, and M. Dijkstra, *Phys. Rev. Lett.* **111**, 015501 (2013).

- [25] P. F. Damasceno, M. Engel, and S. C. Glotzer, *ACS Nano* **6**, 609 (2012), arXiv:1109.1323 [cond-mat.soft].
- [26] M. Ester, H.-P. Kriegel, J. Sander, and X. Xu (AAAI Press, 1996) pp. 226–231.
- [27] F. Pedregosa, G. Varoquaux, A. Gramfort, V. Michel, B. Thirion, O. Grisel, M. Blondel, P. Prettenhofer, R. Weiss, V. Dubourg, J. Vanderplas, A. Passos, D. Cournapeau, M. Brucher, M. Perrot, and E. Duchesnay, *Journal of Machine Learning Research* **12**, 2825 (2011).
- [28] A. B. Harris, R. D. Kamien, and T. C. Lubensky, *Rev. Mod. Phys.* **71**, 1745 (1999).
- [29] J. Henzie, M. Grünwald, A. Widmer-Cooper, P. L. Geissler, and P. Yang, *Nature materials* **11**, 131 (2012).
- [30] L. Rossi, S. Sacanna, W. T. Irvine, P. M. Chaikin, D. J. Pine, and A. P. Philipse, *Soft Matter* **7**, 4139 (2011).
- [31] K. L. Young, M. L. Personick, M. Engel, P. F. Damasceno, S. N. Barnaby, R. Bleher, T. Li, S. C. Glotzer, B. Lee, and C. A. Mirkin, *Angewandte Chemie International Edition* **52**, 13980 (2013).
- [32] V. N. Manoharan, *Science* **349**, 942 (2015).

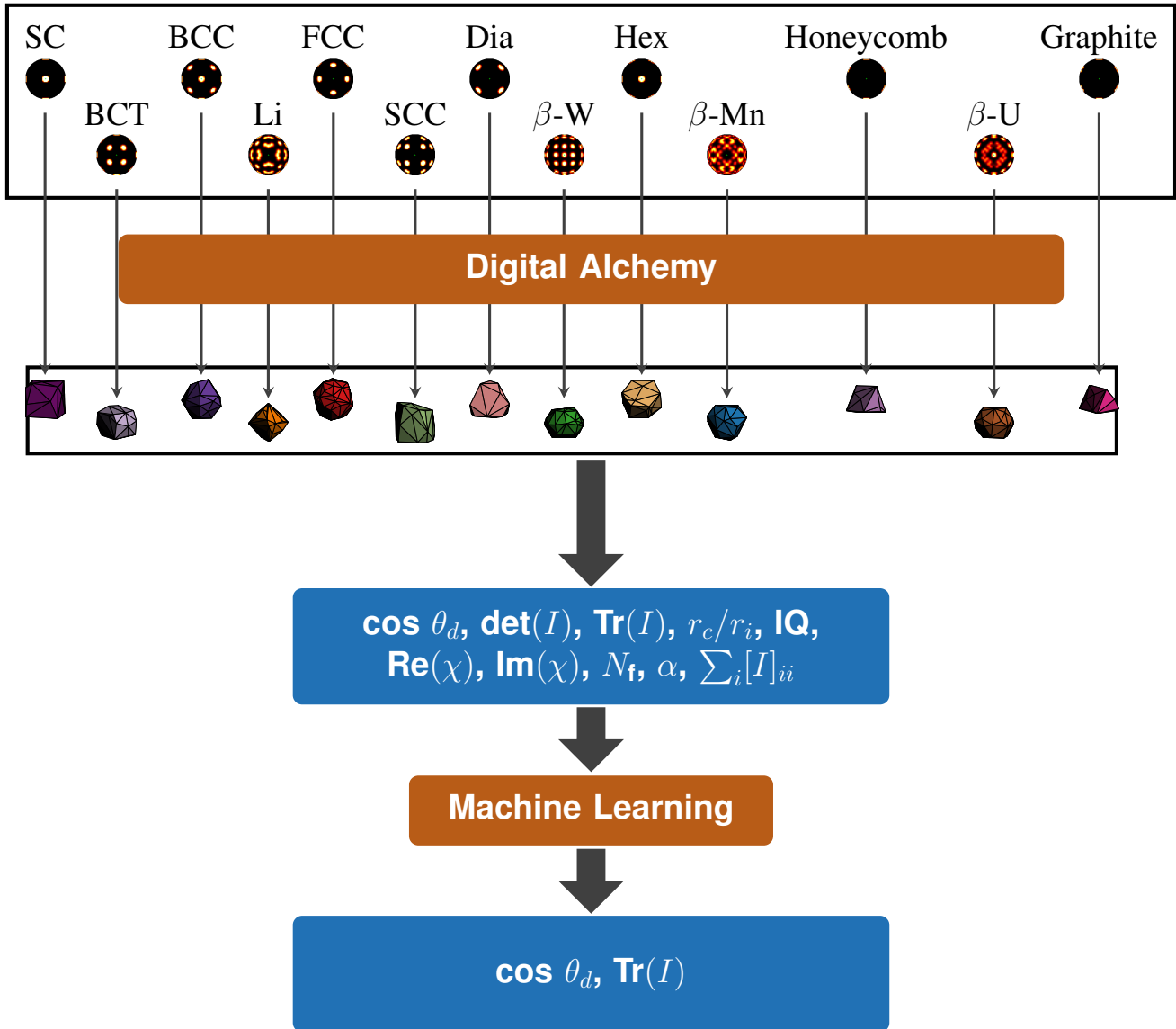


FIG. 1. We use the Digital Alchemy inverse materials design approach to find optimal and near-optimal hard, convex, colloidal, polyhedral shapes for 13 target structures. We use the Random Forest technique from machine learning to classify shapes. We find that, of 10 measures of shape, two – the dihedral angle ( $\cos(\theta_d)$ ) and the trace of the moment of inertia tensor ( $\text{Tr}(I)$ ) – are sufficient to predict the self assembly behavior of a shape.

Correlation	$\cos \theta_d$	$r_c/r_i$	$\det(I)$	IQ	$\text{Re}(\chi)$	$\text{Im}(\chi)$	$N_f$	$\alpha$	$\sum_i [I]_{ii}$	$\text{Tr}(I)$
$\cos \theta_d$	1	0.03	0.02	-0.1	0.01	-0.09	0	0.08	0.02	0.02
$r_c/r_i$	0.03	1	0.51	-0.23	0.04	-0.06	-0.06	0.3	0.52	0.54
$\det(I)$	0.02	0.51	1	-0.51	0.09	-0.03	-0.07	0.58	1	0.99
IQ	-0.1	-0.23	-0.51	1	-0.02	0.27	-0.31	-0.97	-0.5	-0.5
$\text{Re}(\chi)$	0.01	0.04	0.09	-0.02	1	-0.03	0	0.02	0.08	0.08
$\text{Im}(\chi)$	-0.09	-0.06	-0.03	0.27	-0.03	1	-0.14	-0.22	-0.03	-0.03
$N_f$	0	-0.06	-0.07	-0.31	0	-0.14	1	0.21	-0.06	-0.06
$\alpha$	0.08	0.3	0.58	-0.97	0.02	-0.22	0.21	1	0.58	0.57
$\sum_i [I]_{ii}$	0.02	0.52	1	-0.5	0.08	-0.03	-0.06	0.58	1	1
$\text{Tr}(I)$	0.02	0.54	0.99	-0.5	0.08	-0.03	-0.06	0.57	1	1

TABLE I. Correlation matrix of 10 geometric measures for the  $\beta$ -Mn structure.

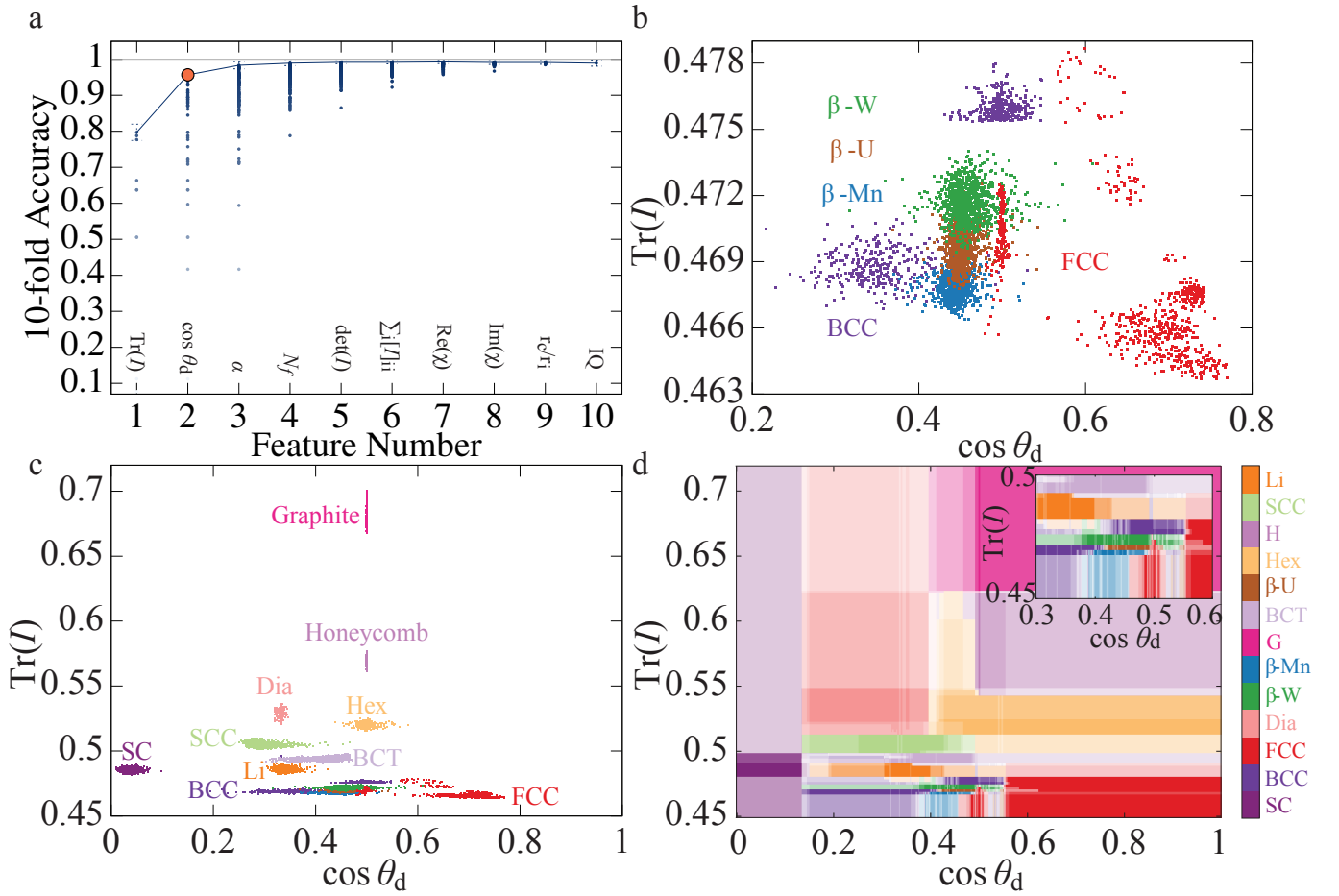


FIG. 2. (a) From low density shape distributions produced via Alch-MC, we classify shapes using combinations of 10 geometric criteria via the random forest method from machine learning. We find that two shape features ( $\cos(\theta_d)$  and  $\text{Tr}(I)$ ) give greater than 91% accuracy in predicting structure. (c) Shape distributions from Alch-MC plotted as a function of the two primary shape features (Including both low density and high density shapes). Each mark represents an observed shape, and is colored by its corresponding crystal structure. Inset shows regions of shape space in which different structures are densely clustered. (b) Zoom in of the densely distributed structure region in (c). (d) Model prediction probability based on particle geometry of self-assembly behavior of hard convex polyhedra that crystallize into 13 target structures.

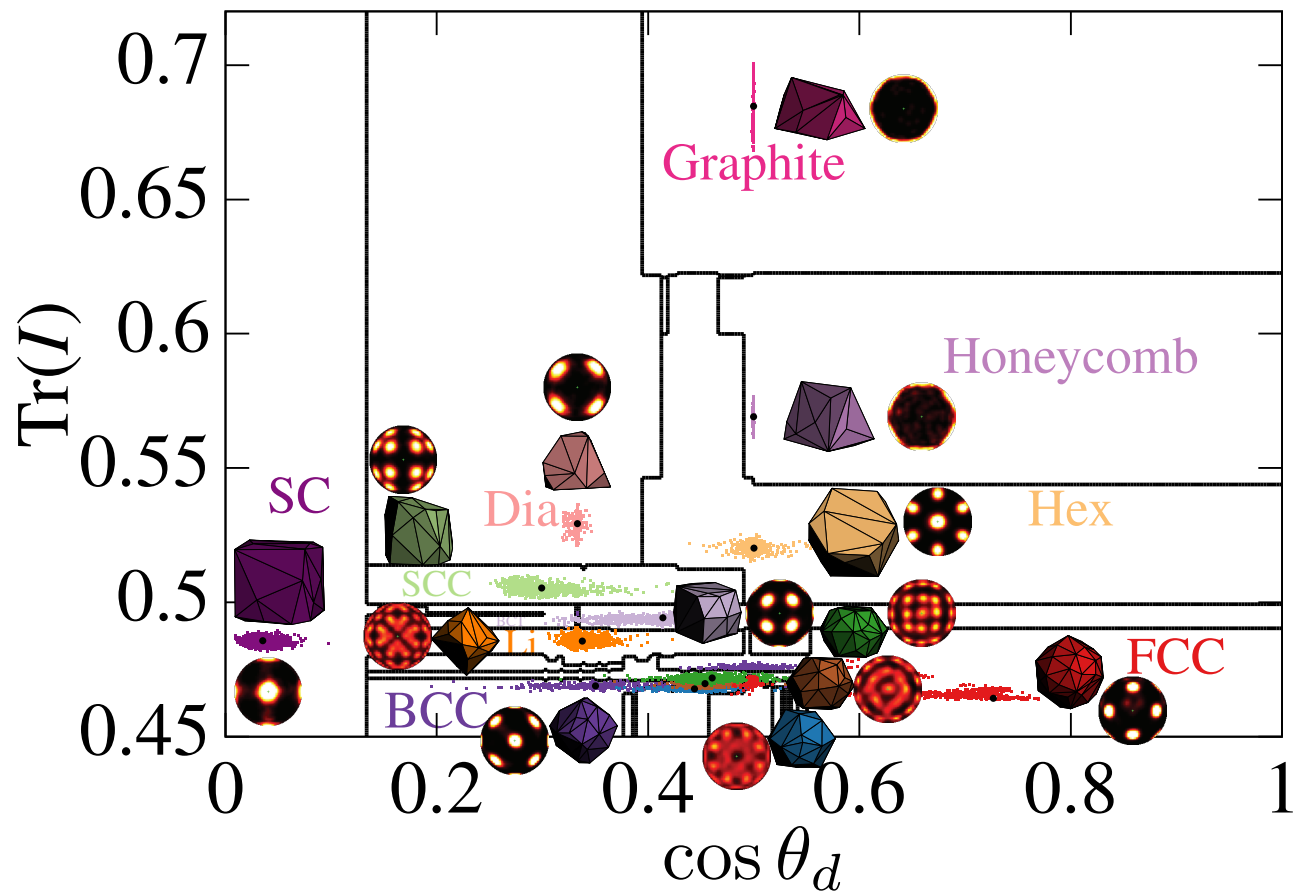


FIG. 3. Model prediction of self-assembly of hard, convex, colloidal polyhedra. Marks indicate observed particle shapes and are colored by structure. Black marks indicate shape distribution peaks corresponding to thermodynamically optimal particle shapes. Example near-optimal particle shapes are shown.

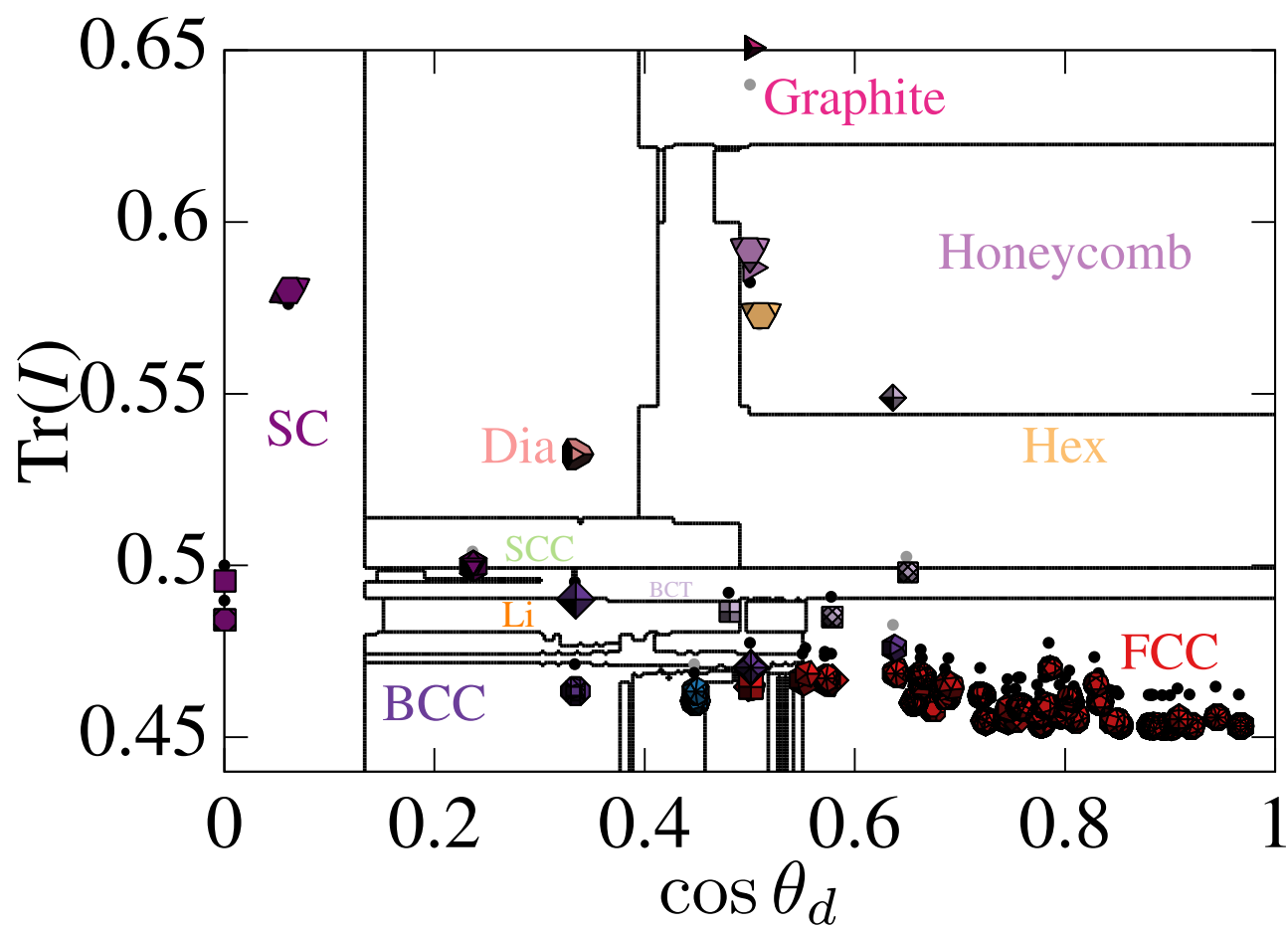


FIG. 4. Test of empirical model prediction against previously reported dataset describing crystal self-assembly of 71 convex polyhedra. Model correctly predicts precise crystal structure observed in self-assembly in 65 of 71 cases (91.55%).